ON-LINE LEARNING OF VIRTUAL IMPEDANCE PARAMETERS IN NON-CONTACT IMPEDANCE CONTROL USING NEURAL NETWORKS

Yoshiyuki Tanaka
Faculty of Information Sciences
Hiroshima City University
Hiroshima, 731-3194 JAPAN
Email: ytanaka@im.hiroshima-cu.ac.jp

Mutsuhiro Terauchi
Faculty of Kansei Information
Hiroshima International University
Hiroshima, 724-0695 JAPAN
Email: mucha@he.hirokoku-u.ac.jp

Toshio Tsuji
Department of Artificial Complex Systems Engineering
Hiroshima University
Hiroshima, 739-8527 JAPAN
Email: tsuji@hfl.hiroshima-u.ac.jp

Makoto Kaneko
Department of Artificial Complex Systems Engineering
Hiroshima University
Hiroshima, 739-8527 JAPAN
Email: kaneko@hfl.hiroshima-u.ac.jp

ABSTRACT

An impedance control method is one of the most effective frameworks to control the interaction between a manipulator and an environment. However, under the conventional method, the manipulator cannot be controlled until the end-effector makes contact with the external environment. For such the problem, a non-contact impedance control has been proposed. This method can regulate not only the end-point impedance but also the virtual impedance that works between the manipulator and the environment by using the visual information. The present paper proposes a method using neural networks to regulate the virtual impedance parameters according to a target task. The validity of the proposed method is verified through the computer simulations of the catching task.

INTRODUCTION

The impedance control (Hogan, 1987) is one of the most important frameworks to control the interaction between a manipulator and an environment. This method can regulate response properties of the manipulator against external disturbances by modifying the mechanical impedance parameters, i.e., inertia, viscosity, and stiffness, to the desired values. However, since no external force is exerted until the end-effector makes contact with the environment, the conventional method is not useful in some cases where no interaction force between the manipulator and its environment exists.

Recently, the vision-based control for robot manipulators has been actively exploited, in which the robot is controlled by using the visual information on the task space. Based on the framework of vision-based control, Castano and Hutchinson (1994) proposed the visual compliance, but do not consider its optimization according to the target task. Also, Tsuji et al. (1999) and Nakabo et al. (1996) have proposed a concept of the virtual impedance using the visual information. Especially, Tsuji et al. have developed a non-contact impedance control method. In this method, the virtual impedance is considered between the end-effector and objects when the objects come into the interior of a virtual sphere set at the tip of the end-effector, so that the virtual force for motion control of the end-effector can be generated before contacting with the objects. In general, however, it is extremely difficult to modify the virtual impedance parameters according to the time-varying characteristics of objects and environments.

On the other hand, there have been many studies that apply a neural network (NN) to the force control and the hybrid control of manipulators (Tokita et. al, 1989)(Tao et. al, 1993)(Kiguchi et. al, 1995), and also the impedance control methods using NN (Gomi et. al, 1993)(Lin et. al, 1997). However, most of such impedance methods regulate the impedance parameters depending on the model uncertainties of the manipulator and the environment or on the external disturbances through the learning of NN with the given desired impedance. To the contrary, some methods using NN try to obtain the suitable impedance according to the task and the environment. For example, Asada (1990) showed that the nonlinear viscosity of the end-effector could be realized by using the NN model as a force feedback controller. Cohen and Flash (1991) proposed a method to regulate the end-effector stiffness and viscosity of the manipulator. In this method, however, the NN cannot regulate an inertia property of the end-effector and only the contact movements can be learned. Also, Yang and Asada (1996) proposed a progressive learning method that can obtain the appropriate impedance parameters by adjusting the desired velocity trajectory. Then, Tsuji et al. (1996, 1999) proposed the iterative learning methods using NNs that can regulate all impedance parameters and the desired end-point trajectory at the same time. However, these learning methods cannot be applied to the task in which the end-effector dose not contact with the environment.

In this paper, an on-line learning method using NNs for the virtual impedance parameters in the non-contact impedance control is proposed by expanding the previous methods (Tsuji et al. 1996, 1999). The present method regulates the virtual impedance through the on-line learning of NNs with an energy function depending on a given task. Besides, the relative velocity during free movements and the interaction force during contact movements can be adapted for the target task. The validity of the method is investigated through computer simulations of the catching-a-ball task by a robotic manipulator.

NON-CONTACT IMPEDANCE CONTROL

Impedance Control

In general, a motion equation of an m-joint manipulator in the l-dimensional task space can be expressed as

$$M(\theta)\ddot{\theta} + h(\theta, \dot{\theta}) = \tau + J^T(\theta)F_{int}, \tag{1}$$

where $\theta \in \Re^m$ is the joint angle vector; $M(\theta) \in \Re^{m \times m}$ is the non-singular inertia matrix (hereafter denoted by M); $h(\theta, \dot{\theta}) \in \Re^m$ is the nonlinear term including the joint torque due to the centrifugal, Coriolis, gravity and friction forces; $\tau \in \Re^m$ is the joint torque vector; $F_{int} \in \Re^l$ is the external force exerted on the end-effector; $J(\theta) \in \Re^{l \times m}$ is the Jacobian matrix (hereafter denoted by J).

The desired impedance properties of the end-effector can be written by

$$M_e d\ddot{X} + B_e d\dot{X} + K_e dX = F_{int}, \tag{2}$$

where $M_e, B_e, K_e \in \Re^{l \times l}$ are the desired inertia, viscosity and stiffness matrices of the end-effector, respectively; and $dX = X_e - X_d \in \Re^l$ is the displacement vector between the current position of the end-effector X_e and the desired one X_d. The impedance control law without an inverse of the Jacobian matrix is given (Hogan, 1987) by

$$\tau = \tau_{effector} + \tau_{comp}, \tag{3}$$

$$\begin{aligned} \tau_{effector} = J^T\{M_x(\theta)[M_e^{-1}(-K_e dX - B_e d\dot{X}) \\ +\ddot{X}_d - \dot{J}\dot{\theta}] - [I - M_x(\theta)M_e^{-1}]F_{int}\}, \end{aligned} \tag{4}$$

$$\tau_{comp} = (M^{-1}J^T M_x(\theta)J)^T \hat{h}(\theta, \dot{\theta}), \tag{5}$$

where $M_x(\theta) = (J\hat{M}^{-1}J^T)^{-1} \in \Re^{l \times l}$ indicates the operational space kinetic energy matrix which is nonsingular as far as the joint configuration θ is not in a singular posture; $\tau_{effector} \in \Re^m$ in (4) represents the joint torque vector to realize the desired end-effector impedance; $\tau_{comp} \in \Re^m$ in (5) is the joint torque vector for nonlinear compensation; $\hat{h}(\theta, \dot{\theta})$ and $\hat{M}$ denote the estimated values of $h(\theta, \dot{\theta})$ and M, respectively; and $I \in \Re^{l \times l}$ is the unit matrix.

Impedance properties of the end-effector can be regulated by employing the designed controller in (3).

Non-contact Impedance Control

Figure 1 shows a schematic representation of the non-contact impedance control (Tsuji et. al, 1996, 1999). Let us consider the case that an object approaches a manipulator, and set a virtual sphere with radius r at the center of the end-effector. When the object comes into the interior of the virtual sphere, the normal vector from the surface of the sphere to the object $dX_o \in \Re^l$ is defined by

$$dX_o = X_r - rn, \tag{6}$$

where $X_r = X_o - X_e$ is the displacement vector from the center of the sphere $X_e \in \Re^l$ (namely, the end-point position) to one of the object $X_o \in \Re^l$; and the vector $n \in \Re^l$ is given by

$$n = \begin{cases} \frac{X_r}{|X_r|} & (|X_r| \neq 0) \\ 0 & (|X_r| = 0) \end{cases} \tag{7}$$

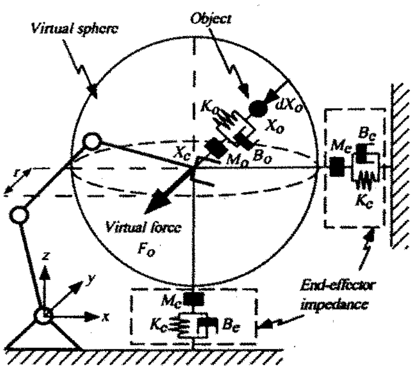

Figure 1. Schematic representation of a non-contact impedance control

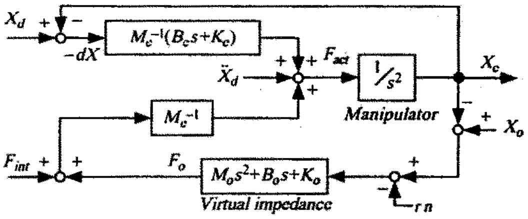

Figure 2. The block diagram of the non-contact impedance control

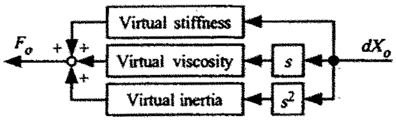

Figure 3. Virtual impedance composed of three components

The virtual impedance works between the end-effector and the object when the object is in the virtual sphere ($|X_r| < r$). At that time, the virtual external force exerted on the end-effector $F_o \in \Re^l$ is given by

$$F_o = \begin{cases} M_o d\ddot{X}_o + B_o d\dot{X}_o + K_o dX_o & (|X_r| < r) \\ 0 & (|X_r| \geq r) \end{cases}, \tag{8}$$

where M_o, B_o and $K_o \in \Re^{l \times l}$ represent the virtual inertia, viscosity and stiffness matrices, respectively. F_o becomes zero when the object is not in the virtual sphere or when the object is at the center of the sphere. Then, the dynamic equation of the end-effector in the non-contact impedance control can be obtained from (2) as

$$M_e d\ddot{X} + B_e d\dot{X} + K_e dX = F_{int} + F_o. \tag{9}$$

Figure 2 shows a block diagram of the non-contact impedance control using (7) and (8). The response of the end-effector position $X_e(s)$ with respect to the object position $X_o(s)$ and the desired end-effector position $X_d(s)$ can be derived as

$$X_e(s) = \frac{R_o(s)}{R(s)} X_o(s) + \frac{R_e(s)}{R(s)} X_d(s) + \frac{-R_o(s)rn + F_{int}(s)}{R(s)}, \tag{10}$$

where $M = M_o + M_e$, $B = B_o + B_e$, $K = K_o + K_e$, $R(s) = Ms^2 + Bs + K$, $R_o(s) = M_o s^2 + B_o s + K_o$, $R_e(s) = M_e s^2 + B_e s + K_e$, respectively. Therefore, the system is stable under $M_o \geq -M_e$, $B_o \geq -B_e$, $K_o \geq -K_e$, where all equal signs in these conditions do never establish at the same time.

In the non-contact impedance control method, the end-effector impedance is modified according to a task as same as the conventional method, while the virtual impedance between the end-effector and the object is regulated for controlling the relative movements. In the present paper, the virtual impedance parameters M_o, B_o, K_o are regulated to the appropriate values for the given task through the learning of NNs.

ON–LINE LEARNING OF VIRTUAL IMPEDANCE BY NNS

Structure of Control System

The proposed control system is constructed by exchanging the virtual impedance part in Fig. 2 for the composition with three multi-layer NNs as shown in Fig. 3; *a virtual stiffness network* (VSN) at K_o, *a virtual viscosity network* (VVN) at B_o, and *a virtual inertia network* (VIN) at M_o. Inputs of the NNs are the relative movements between end-effector and object (X_r, $\dot{X}_r$ and $\ddot{X}_r$) and the interaction force F_{int}, while each of the NNs outputs the corresponding impedance parameter: K_o from the VSN, B_o from the VBN, and M_o from the VIN, respectively.

The NNs utilize a linear function in the input units and a sigmoid function in the hidden and output units as follows:

$$x_i = \begin{cases} I_i & (input\ layer) \\ \sum w_{ij} y_i & (middle\ and\ output\ layers) \end{cases}, \tag{11}$$

$$y_i = \begin{cases} x_i & (input\ layer) \\ \frac{1}{1+e^{-x_i}} & (middle\ layer) \\ \frac{U}{2}\left(\frac{1-e^{-x_i+\theta}}{1+e^{-x_i+\theta}}\right) & (output\ layer) \end{cases}, \tag{12}$$

where x_i and y_i are the input and the output of i-th layer; w_{ij} indicates the weight coefficient from the unit j to i; U and θ are positive constants for the maximum output and the threshold of NN, respectively.

Learning Rule of NNs

The learning of NNs is progressed by means of an energy function $E(t)$ according to a given task, and the synaptic weights w_{ij} in the NNs are modified in the direction of the gradient descent so as to minimize $E(t)$ at each interval time by the weight modification Δw_{ij} as

$$\Delta w_{ij} = -\eta \frac{\partial E(t)}{\partial w_{ij}}, \tag{13}$$

$$\frac{\partial E(t)}{\partial w_{ij}} = \frac{\partial E(t)}{\partial F_{act}(t)} \frac{\partial F_{act}(t)}{\partial O(t)} \frac{\partial O(t)}{\partial w_{ij}}, \tag{14}$$

where η is the learning rate; $F_{act}(t)$ is the control input; and $O(t) \in R^{l \times l}$ indicates the output of NNs. The term $\frac{\partial F_{act}(t)}{\partial O(t)}$ can be computed from Fig. 2 and (7), while $\frac{\partial O(t)}{\partial w_{ij}}$ can be obtained by the error back propagation learning. In the present learning method, the partial differentiation $\frac{\partial E(t)}{\partial F_{act}(t)}$ in (14) is approximated by the finite variations so that the on-line calculation of Δw_{ij} can be carried out by using the changes of $E(t)$ with respect to the slight variation of $F_{act}(t)$.

As designing the energy function $E(t)$ with the end-point position $X_e(t)$ and the velocity $\dot{X}_e(t)$, the term $\frac{\partial E(t)}{\partial F_{act}(t)}$ can be expanded from Fig. 2 as

$$\frac{\partial E(t)}{\partial F_{act}(t)} = \frac{\partial E(t)}{\partial X_e(t)} \frac{\partial X_e(t)}{\partial F_{act}(t)} + \frac{\partial E(t)}{\partial \dot{X}_e(t)} \frac{\partial \dot{X}_e(t)}{\partial F_{act}(t)}. \tag{15}$$

Then, the slight change of the control input $\Delta F_{act}(t)$ yields the following approximations as

$$\Delta X_e(t) \approx \Delta F_{act}(t) \Delta t_s^2, \tag{16}$$

$$\Delta \dot{X}_e(t) \approx \Delta F_{act}(t) \Delta t_s, \tag{17}$$

where Δt_s is the sampling interval. Thus, $\frac{\partial X_(t)}{\partial F_{act}(t)}$ and $\frac{\partial \dot{X}_(t)}{\partial F_{act}(t)}$ can be expressed (Tsuji et. al, 1999) as follows:

$$\frac{\partial X_e(t)}{\partial F_{act}(t)} = \frac{\Delta X_e(t)}{\Delta F_{act}(t)} = \Delta t_s^2 I, \tag{18}$$

$$\frac{\partial \dot{X}_e(t)}{\partial F_{act}(t)} = \frac{\Delta \dot{X}_e(t)}{\Delta F_{act}(t)} = \Delta t_s I. \tag{19}$$

On-line learning of the virtual impedance can be carried out with the derived learning rules (13) ~ (19) under the stable conditions on the non-contact impedance control; i.e., $M_o \geq -M_e$, $B_o \geq -B_e$, and $K_o \geq -K_e$.

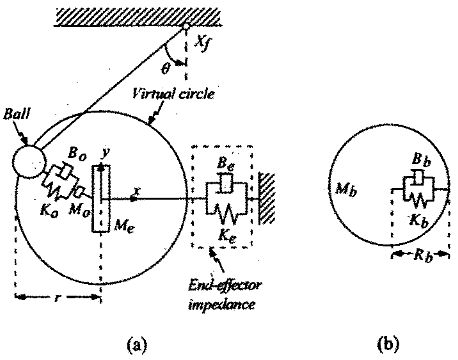

Figure 4. An example of a catching task

APPLICATION TO CONTACT TASKS

A catching-a-ball task is examined as an example of contact tasks by a robotic manipulator, in which the end-effector of the manipulator contacts with an approaching ball and tries to control relative movements as smooth as possible in order to catch the ball. A series of computer simulations was carried out to investigate the effectiveness of the on-line learning of virtual impedance parameters.

Catching-a-ball Task

Figure 4 shows the catching task by the manipulator with one degree-of-freedom ($l = 1$), in which a ball is hung from the ceiling at $X_f = [0.5, 2.1]$ [m] by a pendulum with length $L = 2.1$ [m]. The ball is expressed with a viscoelastic model as shown in Fig. 4 (b), and its properties are set as $B_b = 70$ [Ns/m], $K_b = 2000$ [N/m] with weight $M_b = 0.6$ [kg] and radius $R_b = 0.0322$ [m]. Also, the impedance parameters of the end-effector are set as $M_e = 25$ [kg], $B_e = 200$ [Ns/m], $K_e = 400$ [N/m]. The initial position and the target position of the end-effector, $X_e(0)$ and X_d, are set at the origin of the task space, while the initial angle of the pendulum at $\theta_0 = -\pi/8$ [rad].

In the target task, the virtual impedance works between the end-effector and the ball when the ball comes into the interior of the virtual sphere with radius $r = 0.2$ [m]. The virtual interaction force F_{int} is calculated with the relative position dX_b between the end-effector and the ball by

$$F_{int} = \begin{cases} B_b d\dot{X}_b + K_b dX_b & (|X_r| \leq R_b) \\ 0 & (|X_r| > R_b) \end{cases}, \tag{20}$$

where $dX_b = X_r - R_b n$; and X_r represents the vector from the end-effector to the center of the ball.

The manipulator should be controlled to avoid exerting a large interaction force on its end-effector and the ball without overshooting. For that, it can be suggested not only controlling the end-point force after contacts with the ball but also reducing the relative velocity between the end-effector and the approaching ball beforehand. Accordingly, an energy function for the learning of NNs can be designed as

$$E(t) = E_v(t) + \mu E_f(t), \tag{21}$$

$$E_v(t) = \frac{1}{2}(\alpha(X_r)\dot{X}_r(t_i) - \dot{X}_r(t))^2, \tag{22}$$

$$E_f(t) = \frac{1}{2}\int_0^t (F_d(u) - F_{int}(u))^2 du, \tag{23}$$

where t_i denotes the contact time just when the ball contacts with the virtual sphere; F_d indicates the desired interaction force; and $\alpha(X_r)$ is the time-varying gain function to smooth the changes of velocity immediately after the ball enters the virtual sphere defined by

$$\alpha(X_r) = \begin{cases} \sin \frac{(|X_r| - R_b)\pi}{2(r - R_b)} & (|X_r| \geq R_b) \\ 0 & (|X_r| < R_b) \end{cases}. \tag{24}$$

The on-line learning needs the partial differential computations in (14) by every sampling interval. In the target task, the term $\frac{\partial E(t)}{\partial F_{act}(t)}$ in (14) can be derived by means of (18) and (19) with the energy function in (21) ~ (23) as follows:

$$\frac{\partial E(t)}{\partial F_{act}(t)} = \frac{\partial E_v(t)}{\partial F_{act}(t)} + \mu \frac{\partial E_f(t)}{\partial F_{act}(t)}, \tag{25}$$

$$\frac{\partial E_v(t)}{\partial F_{act}(t)} = \Delta t_s \frac{\partial E_v(t)}{\partial \dot{X}_r(t)}, \tag{26}$$

$$\frac{\partial E_f(t)}{\partial F_{act}(t)} = \Delta t_s^2 \frac{\partial E_f(t)}{\partial X_r(t)} + \Delta t_s \frac{\partial E_f(t)}{\partial \dot{X}_r(t)}. \tag{27}$$

The learning of the NNs for the target task is carried out with the above approximations.

Computer Simulations

In the computer experiments, the VSN, VVN and VIN were of four layered networks with four input units, two hidden layers with twenty-five units and one output unit; the initial values of the synaptic weights w_{ij} were randomly chosen under $|w_{ij}| < 0.05$; the learning rates of the NNs were $\eta_p = 0.1$ for VSN, $\eta_v = 1.0$ for VVN, and $\eta_a = 1.0^{-4}$ for VIN, respectively; the sigmoid functions in the output units were adjusted in such a way that output values of the NNs were within -1000 ~ 1000, that is, $U = 2000$ in (12); the synaptic weights were modified five times in every sampling interval; and the constant μ of $E(t)$ in (21) was set at $\mu = 1.0 \times 10^{-3}$.

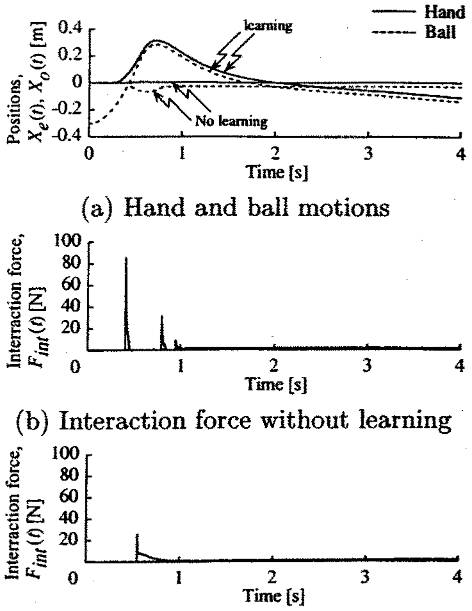

(a) Hand and ball motions

(b) Interaction force without learning

(c) Interaction force with real-time learning

Figure 5. Simulation results of the catching-a-ball task

Figure 5 shows the simulation results with and without real-time learning under the desired interaction force $F_d = 2$ [N]. The figure (a) shows the trajectories of the end-effector (a solid line) and the ball (a broken line), while the figure (b) and (c) show the time histories of the interaction forces without and with on-line learning, respectively. It can be observed from Fig. 5 that the end-effector under the on-line learning takes avoiding actions before contacts with the approaching ball in order to catch the ball as smooth as possible, and that the end-effector force is almost equal to the desired interaction force after learning.

Finally, the time histories of the virtual impedance parameters K_o, B_o and M_o during the catching task are shown in Fig. 6. Both K_o and B_o increase just after the ball enters the virtual sphere, so that the manipulator can moderate the impact force by moving the end-effector toward the opposite direction against the moving direction of ball. Then, K_o reduces to a negative value gradually after contacting the ball, because the end-effector has to move to the positive x direction more than the initial position to realize the desired interaction force. In the same way, M_o becomes a negative value to improve the motion ability of the end-effector with reduction of the equivalent inertia property of the end-effector $M = M_o + M_e$ in (10). Note that the stable conditions $M_o \geq -M_e$ and $K_o \geq -K_e$ are fulfilled in all cases.

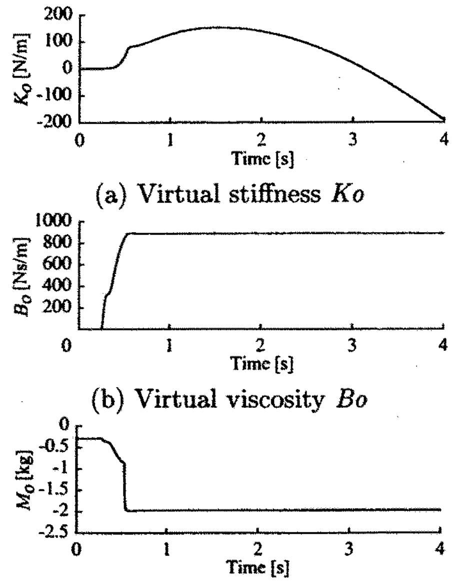

(a) Virtual stiffness *Ko*

(b) Virtual viscosity *Bo*

(c) Virtual inertia *Mo*

Figure 6. Change of the virtual impedance parameters during the catching-a-ball task

CONCLUSION

The present paper has proposed the on-line learning method using NNs for regulating the virtual impedance parameters in the non-contact impedance control. The proposed method can modify the virtual impedance in the desired values by minimizing the energy function according to the given task by the learning of NNs. The validity and feasibility of the proposed method have been confirmed through the computer simulations of the catching task by the manipulator.

Future research will be directed to apply the proposed method to more complicated tasks in the multi-dimensional task space. Also, we plan to investigate a parallel learning with the impedance parameters of the end-effector.

ACKNOWLEDGMENT

This work was partly supported by the Scientific Research Foundation of the Ministry of Education, Science, Sports and Culture, Japan (11650450).

REFERENCES

N. Hogan: "Stable Execution of Contact Tasks Using Impedance Control," in Proceedings *the 1987 IEEE International Conference on Robotics and Automation*, pp.1047–1054, 1987.

A. Castano and S. Hutchinson: "Visual Compliance: Task-directed Visual Servo Control," IEEE Transaction on Robotics and Automation, Vol. 10, No. 3, pp. 334-342, 1994.

T. Tsuji and M. Kaneko: "Non-contact Impedance Control for Redundant Manipulator," *IEEE Transaction on Systems, Man, and Cybernetics - PartA*, Vol. 29, No. 2, pp. 184-193, March 1999.

Y. Nakabo, I. Ishii, and M. Ishikawa: "Robot Control Using Visual Impedance," in Proceedings of *the JSME Annual Conference on Robotics and Mechatronics '96*, Vol. B, pp. 999–1002, 1996. (In Japanese)

M. Tokita, T. Mitsuoka, T. Fukuda, and T. Kurihara: "Force Control of Robot Manipulator by Neural Network (Control of One Degree-of-freedom Manipulator)," *Journal of the Robotics Society of Japan*, Vol.7, No.1, pp.47–51, 1989. (in Japanese)

J. M. Tao and J. Y. S. Luh: "Application of Neural Network with Real-time Training to Robust Position/Force Control of Multiple Robots," in Proceedings of *the 1993 IEEE International Conference on Robotics and Automation*, pp.142–148, 1993.

K. Kiguchi, D. S. Necsulescu, T. Fukuda: "Hybrid Control for an Unknown Environment Using Neural Network," *Journal of the Robotics Society of Japan*, Vol.13, No.2, pp.291–296, 1995. (in Japanese)

G. Gomi and M. Kawato: "Neural Network Control for a Closed Loop System Using Feedback-error-learning," *Neural Networks*, Vol.6, No.7, pp.933–946, 1993.

S.-T. Lin and H.-C. Tsai: "Impedance Control with On-line Neural Network Compensator for Dual-arm Robots," *Journal of Intelligent and Robotic Systems*, Vol.18, pp.87–104, 1997.

H. Asada: "Teaching and Learning of Compliance Using Neural Nets: Representation and Generation of Nonlinear Compliance," in Proceedings of *the 1990 IEEE International Conference on Robotics and Automation*, pp.1237–1244, 1990.

M. Cohen and T. Flash: "Learning Impedance Parameters for Robot Control Using an Associative Search Networks," *IEEE Transactions on Robotics and Automation*, Vol.7, No.3, pp.382–390, June 1991.

B.-H. Yang and H. Asada: "Progressive Learning and Its Application to Robot Impedance Learning," *IEEE Transactions on Neural Networks*, Vol.7, No.4, pp.941–952, 1996.

T. Tsuji, K. Ito, and P. G. Morasso: "Neural Network Learning of Robot Arm Impedance in Operational Space," *IEEE Transactions on Systems, Man and Cybernetics, Part B: Cybernetics*, Vol.26, No.2, pp.290–298, April 1996.

T. Tsuji, K. Harada, H. Akamatsu and M. Kaneko: "On-line Learning of Robot Arm Impedance Using Neural Networks," *Journal of the Robotics Society of Japan*, Vol. 17, No. 2, pp. 234-241, 1999. (in Japanese)